Pergamon

Journal of Structural Geology, Vol. 18, Nos 2/3, pp. 311 to 320, 1996

0191-8141/96 $15.00+0.00

0191-8141(95)00088-7

Effects of propagation rate on displacement variations along faults

D. C. P. PEACOCK

Department of Geological Sciences, University of Plymouth, Drake Circus, Plymouth PL4 8AA, U.K.

and

D. J. SANDERSON

Geomechanics Research Group, Department of Geology, University of Southampton, Southampton Oceanographic Centre, Empress Dock, European Way, Southampton SO14 3ZH, U.K.

(*Received* 9 *December* 1994; *accepted in revised form* 1 *June* 1995)

Abstract—Field observations indicate that much of the variability in the displacement–distance (d–x) profiles and length–displacement relationships of faults is caused by factors which can affect the propagation of faults. These factors include the interaction and linkage of segments, fault bends, conjugate relationships and lithological variations. Existing models for the d–x profiles of faults do not take these effects into account. Fault development can be modelled assuming faults accumulate displacement by a series of slip events, and using a function (p) to describe the rate of fault propagation. When p is constant during fault development, an approximately linear d–x profile eventually develops. When p decreases, such as when interaction occurs, the d–x profile rises above the linear profile. When p increases, the d–x profile initially falls below the linear profile. Such variations in finite d–x profiles mean that the analysis of finite fault displacement gives little information about the d–x profiles of individual slip events.

Variations in p cause variations in r/d_{MAX} ratios (where r is the distance between the maximum displacement point and the fault tip, and d_{MAX} is maximum displacement). Interaction tends to hinder propagation, but displacement continues to increase, causing relatively low r/d_{MAX} ratios. Inelastic deformation can occur at fault tips, especially where strain is concentrated at oversteps, causing steep d–x profiles and low r/d_{MAX} ratios to develop.

INTRODUCTION

Displacement–distance (d–x) profiles (Fig. 1) are useful in describing the displacement characteristics of faults (Muraoka & Kamata 1983, Williams & Chapman 1983). d–x profiles have also been used to interpret the development of faults, using theoretical slip profiles for isolated (Pollard & Segall 1987, Walsh & Watterson 1987, Cowie & Scholz 1992a) or interacting (Bürgmann *et al.* 1994) faults. The r/d_{MAX} ratio (where r = distance between the maximum displacement point and the fault tip, and d_{MAX} = maximum displacement) is also useful in interpreting fault development (Walsh & Watterson 1988, Cowie & Scholz 1992b, Gillespie *et al.* 1992, Dawers *et al.* 1993). Previous models for fault d–x profiles and r/d_{MAX} ratios have attempted to produce 'ideal' characteristics for isolated faults (e.g. Pollard & Segall 1987, Walsh & Watterson 1987, Cowie & Scholz 1992a,b. Gillespie *et al.* 1992). These models do not explain the variability of data for natural faults (Figs. 1c & d) because they do not consider factors which cause variations in fault propagation rates. These factors include the interaction and linkage of segments, fault bends, conjugate relationships and lithological variations (Peacock 1991, Bürgmann *et al.* 1994).

The aim of this paper is to produce a model which accounts for the observed variability in displacement data. Much of the variability can be explained by variations in the rate of propagation of faults. Simple numerical modelling was undertaken to explain observations made during detailed mapping of overstepping faults (Peacock 1991, Peacock & Sanderson 1991, 1994) (Figs. 1 and 2). Displacements have been measured in the field using the separation of marker beds. These displacements are compared with mathematical models which relate displacement to distance along a fault trace. The d–x profiles and r/d_{MAX} ratios are used to explore the importance of propagation rate, particularly the role of fault oversteps.

PREVIOUS MODELS FOR FAULT DISPLACEMENTS

Three models are described here which account for the d–x profiles of 'isolated' faults, i.e. faults which do not interact with other faults and so propagate freely. These models are described because elements of each are used to develop a model for faults which interact with other faults and so do not propagate freely. The modelling of Bürgmann *et al.* (1994) is also mentioned because it gives reasons other than variations in propagation rate for displacement variations along faults. A summary of each model is given in Table 1.

Table 1. Summary of the main features of the various models for fault d–x profiles and r/d_{MAX} ratios

Model	Rationale	d–x Profile	r/d_{MAX} Ratio
Single slip event in an ideal elastic material (Pollard & Seagall 1987)	Displacement depends on the driving stress, the elastic properties of the rock, fault length and the distance from the fault centre	Semi-circular	Controlled by the driving stress and the elastic properties of the rock
Cumulative slip model (Walsh & Watterson 1987)	Displacement builds up by a series of slip events, each obeying the ideal elastic model	Approximately linear after about 100 slip events	$r^2 \propto d_{MAX}$
Post-yield fracture mechanics model (Cowie & Scholz 1992a,c)	Inelastic deformation occurs at fault tips	Approximately semi-circular, but tapering at fault tips	Cowie & Scholz suggest that $r \propto d_{MAX}$
Modelling of Bürgmann *et al.* (1994)	Displacement is controlled by several factors (frictional strength along faults, spatial stress variations, inelastic deformation at fault tips and variations in the elastic modulus of the wall-rocks)	The d–x profiles can be modified by the mechanical factors	The r/d_{MAX} ratios vary, depending on the mechanical factors
Varying propagation rate (this paper)	Displacement builds up by a series of slip events, each with displacement proportional to fault length. Propagation rate can vary during fault development	Varies depending on the propagation history	Varies depending on the propagation history

Model for a single slip event in an ideal elastic material

Pollard & Segall (1987) present a model for a crack subject to mode III loading. Displacement (d) is given by:

$$d = A\,(r^2 - x^2)^{0.5} \quad (1)$$

where A = constant dependent on the driving stress and on the elastic properties of the rock, r = crack half length, and x = distance from the crack centre. Maximum displacement (d_{MAX}) occurs at the crack centre ($x = 0$) and is proportional to crack length. Since $d_{MAX} = Ar$, equation (1) normalizes to a circle, thus:

$$D = (1 - X^2)^{0.5} \quad (2)$$

where D = normalized displacement (d/d_{MAX}) and X = normalized distance from the point of maximum displacement (Fig. 1).

There are three problems with this model. First, ideal elastic behaviour implies infinitely high stresses at crack tips, which is unrealistic because rocks have a finite strength (Cowie & Scholz 1992a). Secondly, faults build up displacement by a series of slip events (Walsh & Watterson 1987), but the model does not account for the propagation of faults or for multiple slip events. Thirdly, the model does not take fault interaction and linkage into account. Pollard & Segall (1987, figs. 8.20 and 8.21) use the example of a dyke segment which oversteps with adjacent dykes. The other dyke segments in the array usually show d–x profiles which are very different from the profile expected for a single displacement (either shear or opening) event in an ideal elastic material. Data for fault segments usually lie below the theoretical profile (Fig. 1c).

The cumulative slip model of Walsh & Watterson (1987)

The Walsh & Watterson (1987) model assumes that a propagating, isolated, planar fault accumulates displacement according to the model for a single slip event in an elastic material, with the amount of incremental slip being proportional to fault length. Walsh & Watterson (1987) predict the following D–X (normalized) relationship:

$$D = 2(1 - X)\,(((1 + X)/2)^2 - X^2)^{0.5}. \quad (3)$$

After many slip events, this profile (Fig. 1c) approximates the linear C-type profile (Fig. 1b) of Muraoka & Kamata (1983), who observe that such profiles are typical of faults in homogeneous rocks.

An advantage of the Walsh & Watterson (1987) model is that it emphasizes the role of multiple slip events. There are, however, two remaining problems. Firstly, it does not account for the variability of d–x profiles that occur. Such variability is illustrated by Walsh & Watterson (1987, fig. 5a) and by Figs. 1(c) & 1(d). Secondly, the model uses equal amounts of fault propagation for each slip event (Walsh & Watterson 1987, figs. 3 and A1) (Fig. 3a). This means that there is the same propagation for early small slip events as for later large slip events, so the r/d_{MAX} ratio decreases with each slip event (see below). The model gives a $d_{MAX} \propto r^2$ relationship, which is not compatible with available data (e.g. Gillespie *et al.* 1992).

The post-yield fracture mechanics model of Cowie & Scholz (1992*a*)

This model involves inelastic deformation during fault growth (also see Cowie & Scholz 1992c, Dawers *et al.* 1993, Scholz *et al.* 1993). Inelastic deformation occurs at the fault tip if the yield strength is exceeded, with yield continuing until stress at the tip just equals the yield strength. The d–x profile for a single slip event in an ideal elastic material is thereby modified, with displacement tapering gradually to the tip. Cowie & Scholz (1992a) argue that their model predicts a linear relationship

between r and d_{MAX}. An advantage of the Cowie & Scholz (1992a) model is that inelastic deformation at fault tips is more realistic than the model for a slip event in an ideal elastic material, which implies infinitely high displacement gradients at fault tips.

Although Cowie & Scholz (1992a,c) state that faults grow by repeated earthquakes, and that total displacement on a fault is the sum of many slip events, they do not demonstrate their conclusion that faults maintain self-similar d–x profiles. The model does not deal with variations in propagation rate. For example, Cowie & Scholz (1992a, fig. 8a) describe the Wasatch Fault, which shows the start of inelastic deformation ('inflection point') at an overstep, so may have been *caused* by the overstep. The best exposed, and the only unsegmented, example they give (their fig. 8c) has a linear d–x profile, with no inflection point. The faults described by Dawers *et al.* (1993, fig. 2) often have asymmetric d–x profiles, and often have M-type profiles (Fig. 1b). This indicates variations in propagation rate by such factors as fault interaction and lithological variations (Peacock 1991, Peacock & Sanderson 1991).

The modelling of Bürgmann et al. (1994)

Bürgmann *et al.* (1994) model the effects of fault geometries, lithological variations and boundary conditions on slip distributions. They show that the d–x

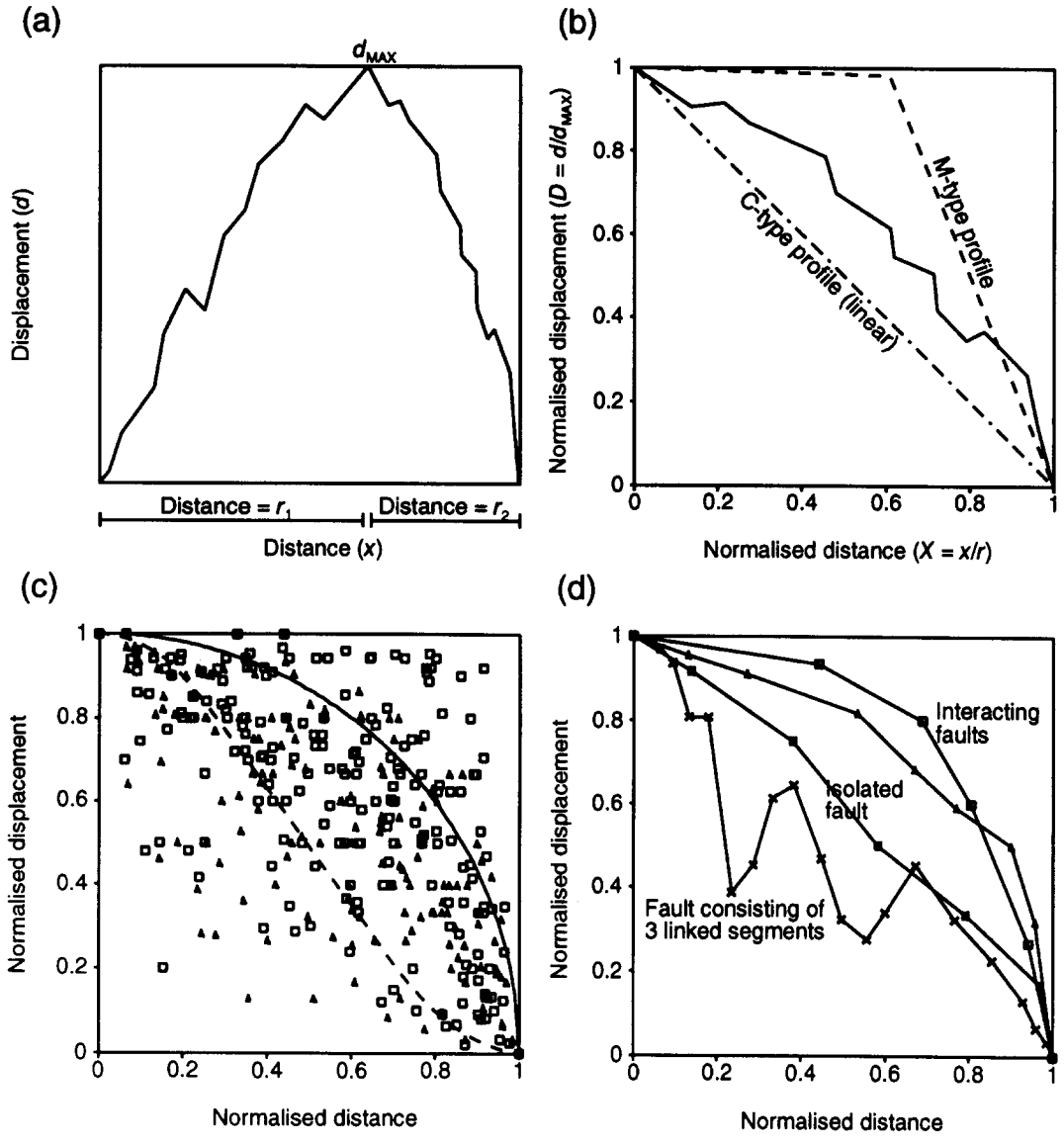

Fig. 1. (a) Displacement–distance (d–x) profile for a fault, showing the maximum displacement (d_{MAX}) and the distance between the maximum displacement point and the tip (r). Note that d_{MAX} is not at the centre of the trace, so $r_1 > r_2$. (b) Normalized displacement–distance (D–X) graph for the right-hand part of the fault in Fig. 1(a). Data are normalized from the point of maximum displacement to the tip, so each fault can have two lines on a D–X (normalized) graph. Normalization has the advantage that the displacement variations along either side of an asymmetric fault, or faults of different sizes, can be compared. The C-type (linear) and M-type profiles of Muraoka & Kamata (1983) are also shown. (c) The (D–X) (normalized) data for strike-slip faults near Kirkcudbright, SW Scotland (open squares, $n = 285$ from 30 segments), and for normal fault segments at Kilve, Somerset (triangles, $n = 245$ from 29 segments). The d–x profiles for a single slip event in an elastic material (solid line) and for the Walsh & Watterson (1987) model (dashed line) are also shown. (d) Examples of (D–X) (normalized) plots for individual fault segments in a fault zone at Kilve. Differences in these d–x profiles can be related to their linkage characteristics (see Peacock & Sanderson 1991).

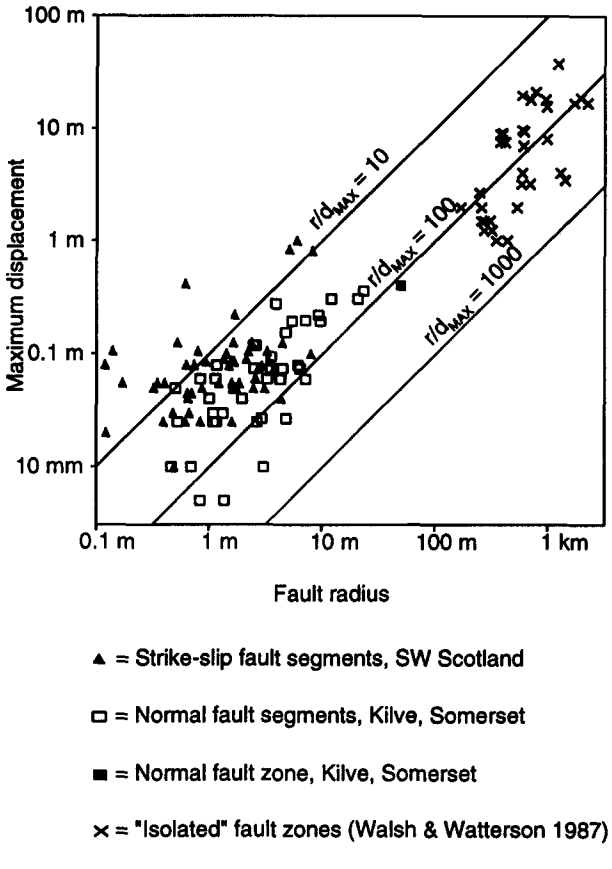

Fig. 2. Graph of r against d_{MAX} (where r = distance between the point of maximum displacement and the fault tip, and d_{MAX} = maximum displacement). Each fault can have two points on this graph, each point representing one side of the fault trace from the maximum displacement point. The scatter of points illustrates the variability in r/d_{MAX} data. Open squares = strike-slip fault segments from Kirkcudbright (n = 55, Peacock 1991); triangles = normal fault segments from Kilve, Somerset (n = 43; Peacock & Sanderson 1991); filled square = normal fault zone from Kilve (n = 1; Peacock & Sanderson 1991); crosses = British coalfield normal faults (n = 34; Walsh & Watterson 1987). The strike-slip fault segments at Kirkcudbright have a mean r/d_{MAX} ratio of 24.2 (range 1.34–109), while the normal fault segments at Kilve have a mean r/d_{MAX} ratio of 65.3 (range 10–307). These are much lower than the mean r/d_{MAX} ratio of 143 for isolated British coalfield normal faults (Walsh & Watterson 1987), probably because interaction causes relatively low r/d_{MAX} ratios on fault segments (Peacock 1991).

profile of a single slip event can be modified by changes in frictional strength along faults, spatial variations in the stress field, inelastic deformation at fault tips and by variations in the elastic modulus of the wall-rocks. They emphasize the importance of segment interaction in causing stress variations and inelastic deformation. Bürgmann *et al.* (1994) suggest that these mechanical factors control the r/d_{MAX} ratios of faults. A problem with the modelling of Bürgmann *et al.* (1994) is that it does not include the effects of fault propagation, but is limited to individual slip events.

MODEL FOR THE DEVELOPMENT OF A PROPAGATING FAULT

The variability in displacement–distance profiles (Fig. 1) and r/d_{MAX} ratios (Fig. 2) illustrates that fault development is more complex than predicted by the models of Pollard & Segall (1987), Walsh & Watterson (1987) and Cowie & Scholz (1992a). The 'isolated' faults these models describe are rare, so interaction between faults should be considered. To model the development of a fault, we assume that a fault builds up displacement by a series of slip events (Fig. 3b), each of which has the d–x characteristics of a fracture in an ideal elastic material [equation (1)]. Thus:

$$d = (c_1^2 - x^2)^{0.5} + (c_2^2 - x^2)^{0.5} \ldots (c_n^2 - x^2)^{0.5} \quad (4)$$

where d = total displacement on a fault, c_1 = initial half length of the fault, $c_n = (c_{n-1}\, p)$, n = number of slip events, and x = distance from fault centre. Equation (4) can be re-written, using p = function for the increase in length of fault, thus:

$$d = \sum_{n=0}^{N} ((p^n c_1)^2 - x^2)^{0.5}. \quad (5)$$

The function p is a parametric representation of fault growth, which we call the *fault propagation rate*. Note that p is not the 'true' rate, i.e. it is not measured with

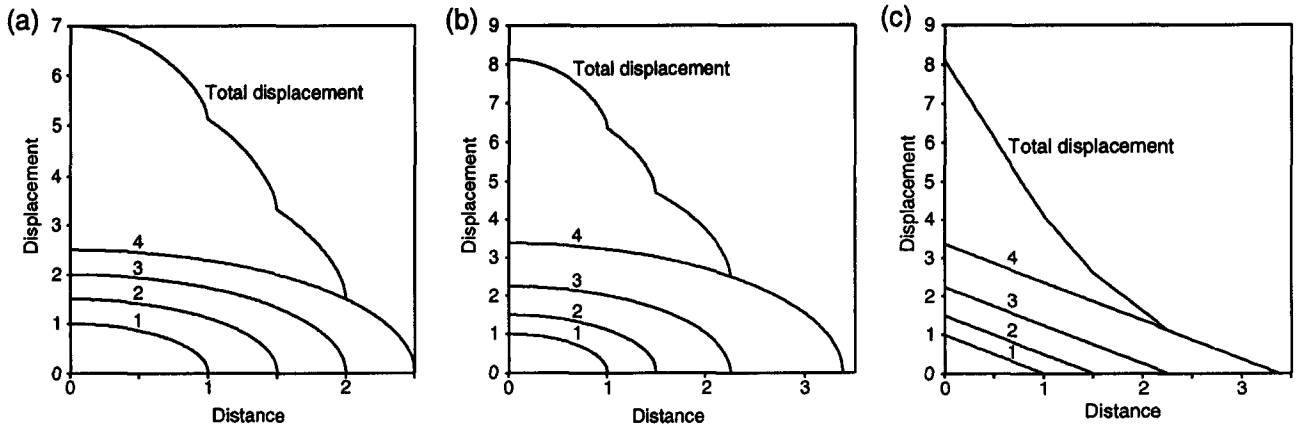

Fig. 3. Displacement–distance (d–x) graphs for four slip events (numbered 1–4), illustrating how displacement builds up on a fault by a succession of slip events, and how the d–x profile changes during fault development. (a) The Walsh & Watterson (1987) model, where fault length increases by the same amount after each slip event. (b) Model using equation (5), in which the propagation rate p = 1.5. (c) Model using a linear d–x profile for each slip event, in which p = 1.5.

respect to time. When $p = 1$, there is no propagation, but when $p > 1$, the fault propagates (Fig. 3b). For example, when $p = 2$, fault lengths are doubled after each slip increment.

The slip distribution of a fracture in an ideal elastic material is used because it is simple, even though real slip distributions are usually more complex (Cowie & Scholz 1992a, Bürgmann *et al.* 1994). Also, the true d–x profile of each slip event is unknown (see below). It is shown below that the actual profile used for individual slip events has little effect on the modelling. In this modelling, the first slip event has $r = 1$ unit and $d_{MAX} = 1$ unit (so $r/d_{MAX} = 1$), with displacement and fault length increasing with successive slip events. Propagation and displacement are proportional to fault length (Scholz *et al.* 1993). Cowie & Scholz (1992c) believe that faults usually grow by 0.25–2.5% of their previous length, i.e. $p = 1.0025$–1.025. There appears, however, to be no published data on the amount of fault propagates during each slip event, so specific values of p cannot be given.

Models for faults with constant propagation rates

Figure 4 shows D–X (normalized) graphs for models of faults with propagation rates (p) of 2, 1.1, 1.01 and 1. The different propagation rates produce different D–X (normalized) graphs. For $p = 2$, the D–X (normalized) profile rapidly falls beneath the profile for a single slip event, to become approximately linear. The fall is slower for $p = 1.1$, but it has become approximately linear after 100 slip events. The profile for $p = 1.01$ has fallen, but is not yet linear after 100 slip events. For $p =$

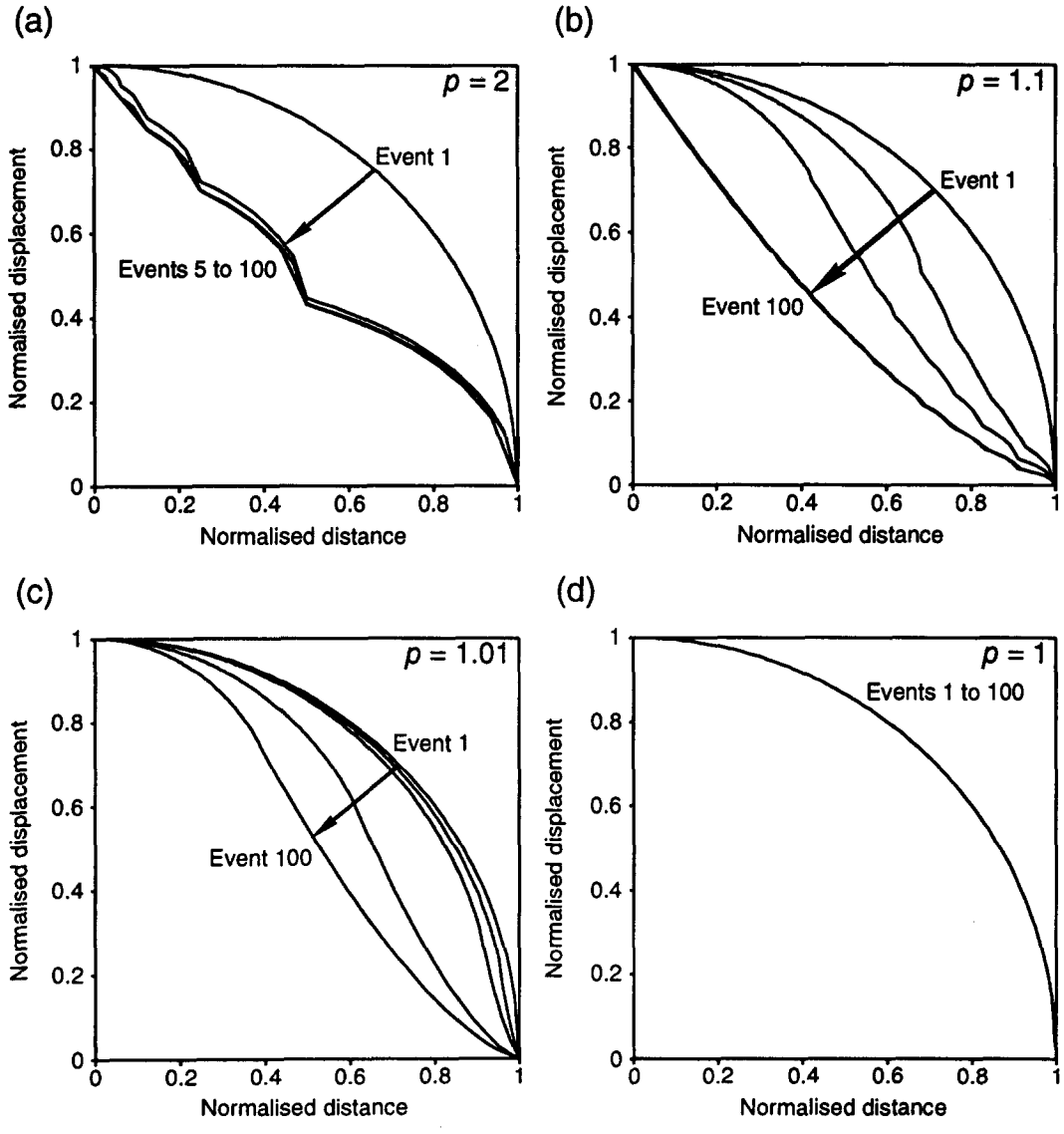

Fig. 4. Normalized displacement–distance (D–X) graphs for different propagation rates (p), illustrating the effect of p on displacement–distance profiles. Each graph shows profiles for 1, 5, 10, 50 and 100 slip events. (a) The D–X graph for $p = 2$. The profile is approximately linear after only a few slip events. (b) The D–X graph for $p = 1.1$. The profile is approximately linear after 100 slip events. (c) The D–X graph for $p = 1.01$. The profile has not yet become linear. (d) The D–X graph for $p = 1$, for 1–100 slip events. If the fault does not propagate, the D–X (normalized) profile does not change, but displacement builds up on the fault (Sibson 1989, fig. 10).

1, fault length is constant but displacement increases on the fault, so the d–x (non-normalized) profile changes. The D–X (normalized) profile, however, does not change. It is probable that profiles for all faults with a constant p value of more than one would eventually become approximately linear.

Effects of variations in propagation rate during fault development

Propagation rate (p) can decrease because of interaction with adjacent faults (Aydin & Schultz 1990), fault bends, conjugate relationships and lithological variations (Peacock 1991). Figure 5(a) shows the case where the propagation rate decreases from $p = 1.1$ for the first 100 slip events, to $p = 1$ for the next 100 slip events, i.e. the fault stops propagating after 100 slip events but displacement continues to increase. After slip event 100, the D–X (normalized) profile (Fig. 5b) arcs upwards from being approximately linear, towards the profile for a single slip event. Such a decrease in p may explain some of the data above the linear profile (Fig. 1c). When p increases from $p = 1.01$ for the first 100 slip events to $p = 1.1$ for the next 100 slip events, the D–X (normalized) profile falls beneath the linear profile, but eventually comes back to approximately linear (Fig. 5c). Such an increase in p may explain some of the data below the linear profile in Fig. 1(c).

An important implication of this modelling is that the final d–x profile is strongly influenced by the propagation history of the fault, and non-elliptical displacement patterns at fault tips are commonly produced (Figs. 4 and 5). The final slip event has only a limited affect on the d–x profile, particularly for faults with low propagation rates (p). This means that the final d–x profile of a fault cannot be used to determine the d–x profile of an individual slip event, as is done by Cowie & Scholz (1992a,c).

Model for two interacting faults

Aydin & Schultz (1990) show that interaction with adjacent faults causes variations in propagation rate, with a tendency for the rate to decrease as faults interact. Figure 6 shows the d–x profiles for a model of two interacting fault segments. The starting point in the model is $p = 1.1$ for 100 slip events, with distance normalized to 1 and displacement modified to maintain the original r/d_{MAX} ratio of 0.0909 (Fig. 7a). To model interaction between two fault segments, the interacting side of each fault segment has $p = 1$, i.e. no propagation. Displacement (d) is:

$$d = d^* + (ne) \tag{6}$$

where d^* = displacement for $p = 1.1$ for 100 slip events, n = number of slip events when $p = 1$ and e = displacement for a single slip event. For the non-interacting (freely propagating) ends of the two segments, $p = 1.1$ and r is given by:

$$r = r^* (d_{MAX}/(r/d_{MAX})) \tag{7}$$

where r^* = fault length for $p = 1.1$ after 100 slip events. Displacement for the non-interacting ends of the fault is given by:

$$d = d^* (d_{MAX}/(r/d_{MAX})). \tag{8}$$

The non-interacting ends of the faults therefore have constant r/d_{MAX} ratios and constant D–X (normalized) profiles. One possible problem with this model is that displacements on the non-interacting ends of the faults build up by slip events which each have the same displacement, so the amount of displacement in each slip event is not proportional to length. The model (Fig. 6) shows that both overstepping segments have asymmetric d–x profiles, with steep displacement gradients at the overstep. This is similar to d–x data for two overstepping faults shown by Peacock (1991, fig. 10b) and Peacock & Sanderson (1991, fig. 11d).

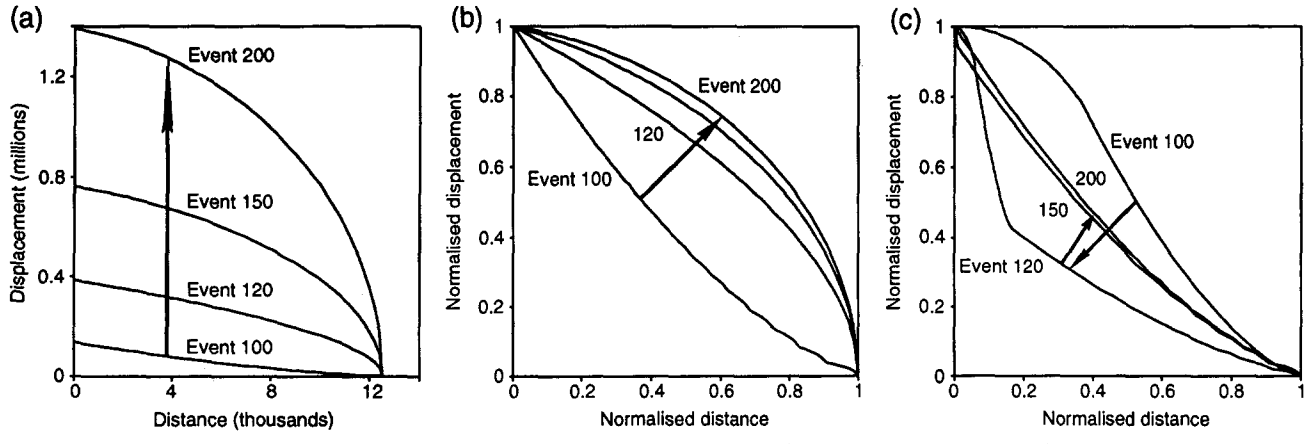

Fig. 5. Graphs illustrating the effects of variations in propagation rate (p). (a) The d–x (non-normalized) profile of a fault where p decreases from $p = 1.1$ for the first 100 slip events to $p = 1$ for the next 100 slip events. (b) The D–X (normalized) graph for the model shown in Fig. 5(a). When $p = 1$, the profile rises with successive slip events to become close to the model for a single slip event in an elastic material. (c) Model for the D–X (normalized) profile of a fault where p increases from $p = 1.01$ for the first 100 slip events to $p = 1.1$ for the next 100 slip events. When $p = 1.1$, the profile falls with successive slip events, eventually becoming more linear.

IMPLICATIONS OF THE MODEL FOR LENGTH–DISPLACEMENT RATIOS

Individual populations of faults show a wide range of r/d_{MAX} ratios (Fig. 2). Much of this variability can be explained by variations in fault propagation rates. Figure 7(a) shows a graph of the change in r/d_{MAX} ratios for the models shown in Fig. 4. For $p = 2$, the r/d_{MAX} ratio rapidly reaches a constant value. For p values of less than about 1.01, the r/d_{MAX} ratios do not reach a constant value until $n > 1000$. For $p = 1$, the r/d_{MAX} ratio continues to decrease linearly. If the first slip event has $r = 1$ and $d_{MAX} = 1$, then, after n slip events:

$$r = p^n \tag{9}$$

$$d_{MAX} = (p^n - 1)/(p - 1) \tag{10}$$

$$r/d_{MAX} = (p^{n-1}(p - 1))/(p^n - 1). \tag{11}$$

This means that, as n approaches infinity:

$$r/d_{MAX} \approx (p - 1)/p. \tag{12}$$

For a given material [i.e. when A in equation (1) is constant], small faults and also large faults with high propagation rates have high r/d_{MAX} ratios (Fig. 7a). The r/d_{MAX} ratios reach a constant value which depends upon p, and after a constant ratio is reached, r is linearly related to d_{MAX} (Fig. 7a).

The Walsh & Watterson (1987) model implies that a fault with n slip increments, and a half length (r) of 1 unit, will have:

$$r = n \tag{13}$$

$$d_{MAX} = An/2(1 + n) \tag{14}$$

$$r/d_{MAX} = 2/(A(1 + n)). \tag{15}$$

The Walsh & Watterson (1987) model therefore implies that r/d_{MAX} ratios decrease with each slip event (Fig. 7a). This is unrealistic, because Scholz *et al.* (1993) show that the amount of fault propagation is proportional to fault length and displacement, which is consistent with a constant r/d_{MAX} ratio.

Figure 7(b) shows r/d_{MAX} data for the model of a decrease in fault propagation rate (p) (Fig. 5a). Because $p = 1.1$, the r/d_{MAX} ratio has reached an approximately constant value after the first 100 slip events. The r/d_{MAX} ratio decreases linearly when $p = 1$, however. Figure 7(c) shows r/d_{MAX} data for the model of an increase in p (Fig. 5c). The r/d_{MAX} ratio decreases approximately

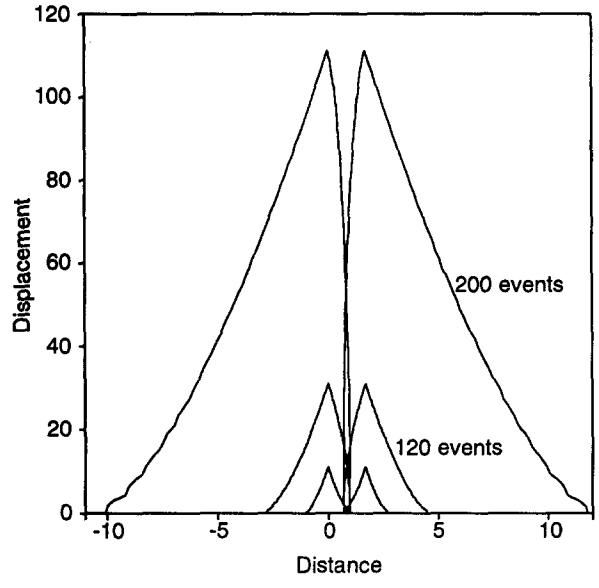

Fig. 6. Model for the d–x profiles of two interacting faults; $p = 1.1$ for the first 100 slip events. Distance is normalized to 1 after the first 100 slip events, and displacement is modified so the r/d_{MAX} ratio is kept constant. An overstep occurs at distance of 0.7–1, where propagation stops, i.e. $p = 1$. The other end of each segment continues to propagate at $p = 1.1$. The d–x graphs are shown for the segments at 100, 120 and 200 slip events. High displacement gradients develop on the faults at the overstep, with the segments showing asymmetric d–x profiles. Linkage between the two segments would produce a composite fault with an irregular d–x profile, often with a displacement minimum at the linkage point (e.g. Ellis & Dunlap 1988).

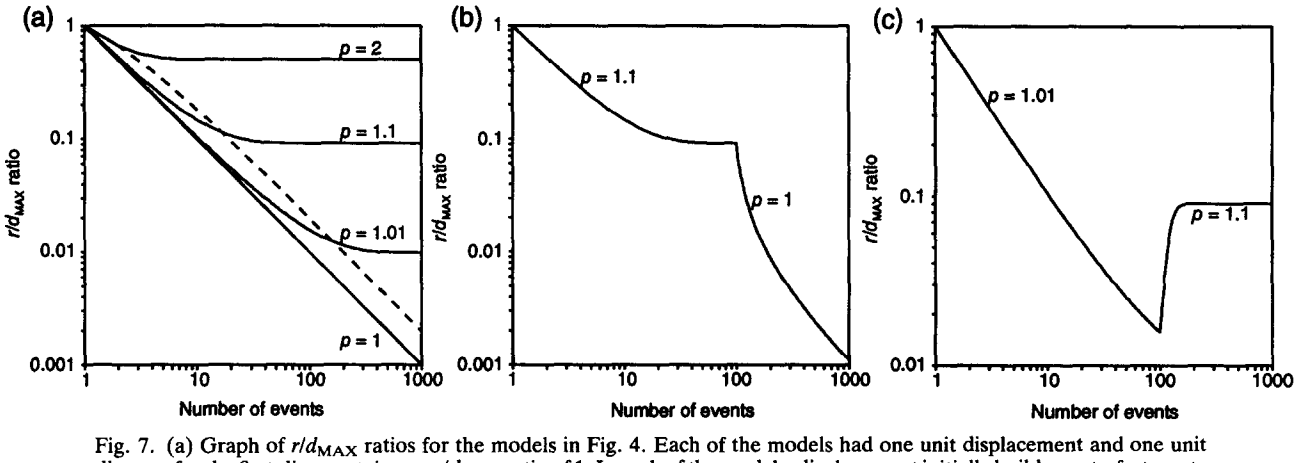

Fig. 7. (a) Graph of r/d_{MAX} ratios for the models in Fig. 4. Each of the models had one unit displacement and one unit distance for the first slip event, i.e. an r/d_{MAX} ratio of 1. In each of the models, displacement initially builds up at a faster rate than fault length, so the r/d_{MAX} ratio decreases (displacement increases in proportion to length). The rate of decrease in the r/d_{MAX} ratio slows as p increases. When $p = 1$, the r/d_{MAX} ratio decreases linearly, but when $p > 1$, a constant r/d_{MAX} ratio is reached. When $p = 2$, the ratio reaches a constant value after about five slip events. The constant r/d_{MAX} ratio occurs at higher values for higher values of p. The dashed line is the r/d_{MAX} ratio for the Walsh & Watterson (1987) model. (b) Graph of r/d_{MAX} ratios for the model shown in Fig. 5(b). The ratio has nearly reached a constant value after the first 100 slip events, but decreases further when p decreases. (c) Graph of r/d_{MAX} ratios for the model shown in Fig. 5(c). The ratio decreases nearly linearly for $p = 1.01$, then increases when p increases.

linearly for the first 100 slip events. The r/d_{MAX} ratio increases when p increases (slip events 101–200). Variations in p therefore cause changes in r/d_{MAX} ratios.

Cowie & Scholz (1992c) consider there to be a 'critical profile', such that fault propagation occurs when the d–x gradient exceeds the critical profile. Scholz *et al.* (1993) suggest that when two faults coalesce, the new r/d_{MAX} ratio is larger than on the two initial segments, so no new propagation occurs until the appropriate ratio is reached. This is not necessary in the model presented in this paper, because a composite fault can continue to propagate at the same rate, eventually reaching the r/d_{MAX} ratio which is relevant to the propagation rate.

DIFFERENT d–x PROFILES FOR INDIVIDUAL SLIP EVENTS

The model used in this paper [equation (5)] is a simplification because post-yield displacement may occur, modifying the d–x profile for each slip event (e.g. Cowie & Scholz 1992b). There are, however, two reasons for using this model. Firstly, it is not clear exactly what form of d–x profile a post-yield fracture mechanics model would have. Such a model would have to include an arbitrary taper of displacement at the fault tip. Secondly, equation (5) is mathematically simple and shows the effects of variations in propagation rate on d–x profiles and r/d_{MAX} ratios.

Figure 8 shows d–x graphs for faults for which a linear d–x profile for each slip event is used (Fig. 3c). The elastic dip model (Figs. 4–7) and the linear model (Fig. 8) have the following features in common.

(1) For a constant propagation rate of $p > 1$, the d–x profile progressively falls beneath the profile for a single slip event, eventually reaching a constant profile (Figs. 4 and 8a).

(2) If propagation stops, the d–x profile rises (Figs. 5b and 8b).

(3) If the propagation rate increases, the d–x profile initially falls (Figs. 5c and 8c).

(4) The r/d_{MAX} ratios are controlled by propagation rate [equation (1)], so are the same for both models. Propagation rate, therefore, has a strong effect on d–x profiles and r/d_{MAX} ratios, whichever model is used for the d–x profile of a single slip event.

EFFECTS OF STRUCTURES AT FAULT OVERSTEPS

The importance of propagation rate on the d–x profiles and r/d_{MAX} ratios of faults, and the effect of fault interaction on propagation rate, have been described above. This section uses the example of oversteps along normal faults in map view to discuss the role of fault oversteps. Such oversteps transfer displacement between segments, effect fault propagation and can cause inelastic deformation (also see Bürgmann *et al.* 1994).

Figure 9 shows a map of two overstepping normal faults. The reorientation of bedding at the overstep is termed a *relay ramp* (Larsen 1988). The relay ramp rotates to transfer displacement between the segments, with the decrease in displacement along one segment being matched by an increase in displacement on the adjacent segment. The rotation can cause steep displacement gradients on the faults at the overstep, producing d–x profiles and r/d_{MAX} ratios which are markedly different from those predicted by the models for isolated faults described above (Peacock 1991, Peacock & Sanderson 1991, 1994).

The steep displacement gradients which often occur in relay ramps indicate that it is somehow easier for displacement to build up on the overstepping faults by the rotation of bedding than by the propagation of the segments. Such propagation would enable the faults to maintain 'average' displacement gradients and r/d_{MAX} ratios, i.e. those which may occur for more isolated

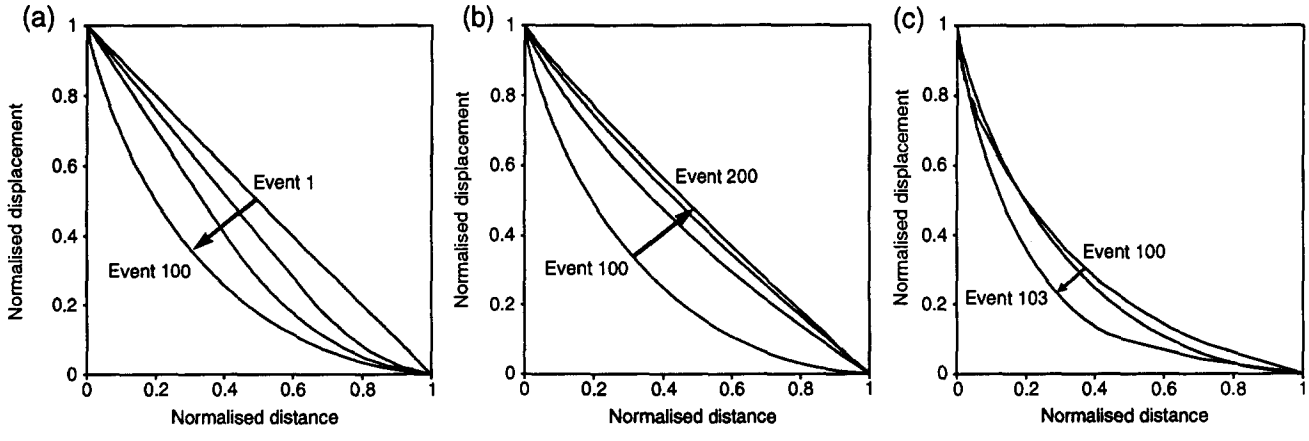

Fig. 8. The D–X (normalized) graphs for faults, assuming displacement builds up by a series of slip events which have linear d–x profiles. (a) Model for a propagation rate (p) of 1.1, for 1, 5, 10, 50 and 100 slip events. As displacement increases, the profile falls below the linear profile, eventually becoming constant. (b) Model for which $p = 1.1$ for the first 100 slip events, and is then reduced to $p = 1$ for the next 100 slip events. The profiles for slip events 100, 120, 150 and 200 are shown. The profile progressively rises towards the linear profile. (c) Model for which $p = 1.1$ for the first 100 slip events, and is then increased to $p = 1.5$ for the next 10 slip events. The profiles for slip events 100, 103 and 110 shown. When p increases, the profile initially falls beneath the constant profile attained when $p = 1.1$.

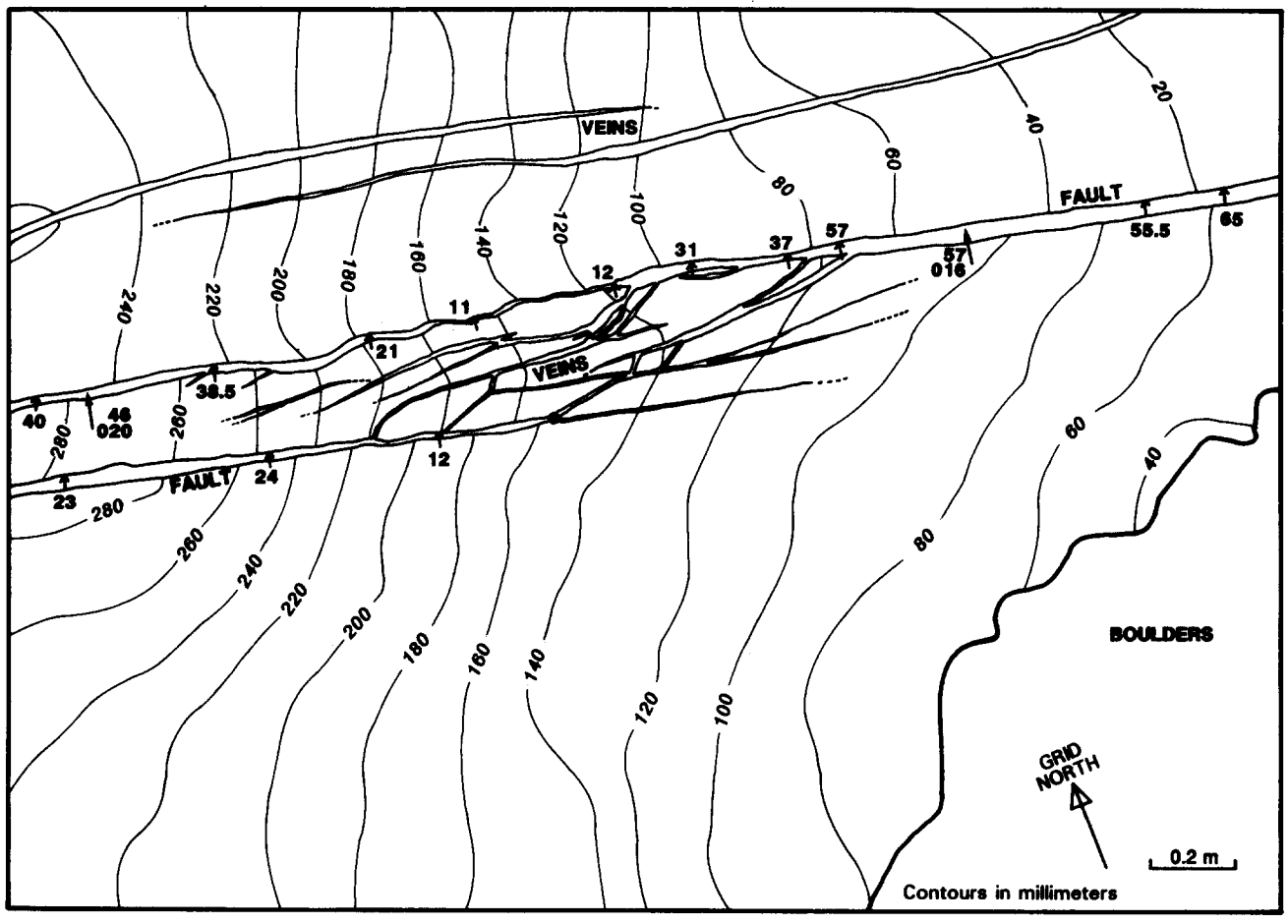

Fig. 9. Map of a relay ramp at Klive, Somerset, U.K. (grid reference ST149446). The contours are for a limestone bedding plane in mm above an arbitrary datum level. Veins and small faults have started to break the ramp. The complex fracturing at the overstep allows high displacement gradients to develop on the faults, and indicates that inelastic deformation occurs (Cowie & Scholz 1992a).

faults. The steep displacement gradients at oversteps, and the low r/d_{MAX} ratios on the overstepping faults, are accommodated by inelastic deformation (Bürgmann *et al.* 1994). This inelastic deformation is indicated by the concentration of veins and minor faults at relay ramps (e.g. Fig. 9). A consequence of inelastic deformation at oversteps is that the d–x profile of a slip event will depart from that of the ideal elastic model (see Cowie & Scholz 1992c), causing complexity in the displacement characteristics of the overstepping fault segments.

Fault zones typically have complex d–x profiles (Figs. 1 and 10), because interaction and linkage produces variability in the segments which form the zone, and because linkage points are usually marked by displacement minima (Peacock & Sanderson 1991, 1994).

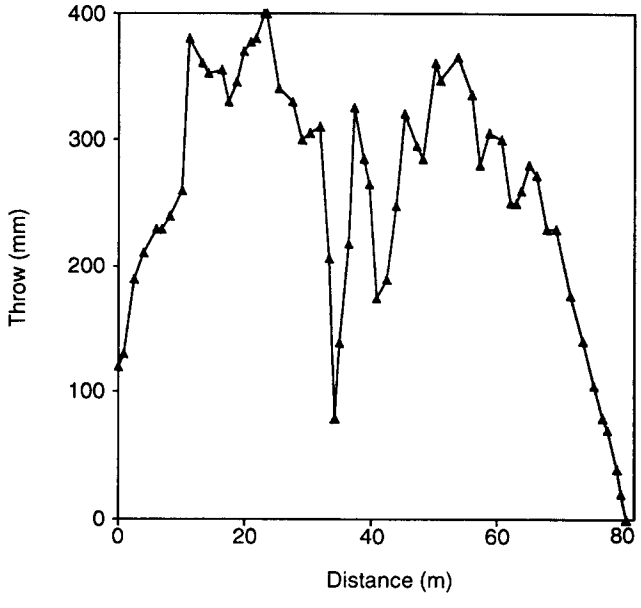

Fig. 10. The d–x graph for a normal fault zone at Kilve, Somerset, U.K. which consists of at least 34 individual fault segments (Peacock & Sanderson 1991). A complex d–x profile results from the interaction and linkage of the segments that form the zone.

CONCLUSIONS

The following conclusions are made from the modelling undertaken in this paper.

(1) Fault development and segment interaction can be modelled using an equation which incorporates variations in fault propagation rates. Variations in propaga-

tion rate can cause much of the variability observed in the d–x profiles and r/d_{MAX} ratios of faults.

(2) Rapidly propagating faults, i.e. those with $p \geq$ about 1.1, develop approximately linear d–x profiles after relatively few slip events, and have relatively high r/d_{MAX} ratios. Slowly propagating faults, i.e. those with $p \leq$ about 1.1, develop approximately linear d–x profiles profiles only after many slip events, and have relatively low r/d_{MAX} ratios.

(3) Variations in propagation rate can be caused by fault interaction, fault bends, conjugate relationships and lithological variations. Interaction with other faults tends to decrease the rate of propagation, causing d–x profiles to rise towards those expected for a single slip event and causing r/d_{MAX} ratios to decrease. A fault segment which interacts with another fault in only one direction typically has maximum displacement away from the centre of the fault trace.

(4) The finite d–x profile is strongly influenced by the propagation history of a fault, so gives little information about the d–x profiles of the individual slip events.

(5) The model presented in this paper explains much of the variability in the r/d_{MAX} ratios of real faults (Fig. 2). The modelling has four consequences: (i) r/d_{MAX} ratios reach a constant value which depends upon p (Fig. 7a), (ii) after a constant ratio is reached, r is linearly related to r/d_{MAX} (Fig. 7a), (iii) the ratio can vary as the propagation rate varies (Figs. 7b & c), (iv) two faults which link do not have to stop propagating until an 'ideal' r/d_{MAX} ratio is reached.

(6) Elliptical and linear d–x profiles for individual slip events cause similar variations in finite d–x profiles and r/d_{MAX} ratios when p varies. Propagation rate therefore appears to have a stronger effect than the d–x profiles for individual slip events.

(7) Veins, minor faults and bed rotation at fault oversteps represent inelastic deformation, causing high displacement gradients to develop on overstepping fault segments.

Variations in propagation rate, caused by such factors as fault interaction, therefore produce complex d–x profiles and variations in r/d_{MAX} ratios. Thus, it is rare for faults to have simple or characteristic d–x profiles or r/d_{MAX} ratios, and any model should be used with caution.

Acknowledgements—Useful reviews were given by Nancye Dawers, Mark Swanson and Steven Wojtal. Emanuel Willemse and Christopher Scholz are thanked for helpful discussions, and David McMullan is thanked for help with equation (5). Funding was provided by the University of Plymouth and the University of Southampton.

REFERENCES

Aydin, A. & Schultz, R. A. 1990. Effect of mechanical interaction on the development of strike-slip faults with echelon patterns. *J. Struct. Geol.* **12**, 123–129.

Bürgmann, R., Pollard, D. D. & Martel, S. J. 1994. Slip distributions on faults: effects of stress gradients, inelastic deformation, heterogeneous host-rock stiffness, and fault interaction. *J. Struct. Geol.* **16**, 1675–1690.

Cowie, P. A. & Scholz, C. H. 1992a. Physical explanation for the displacement–length relationship of faults using a post-yield fracture mechanics model. *J. Struct. Geol.* **14**, 1133–1148.

Cowie, P. A. & Scholz, C. H. 1992b. Displacement–length scaling relationship for faults: data synthesis and discussion. *J. Struct. Geol.* **14**, 1149–1156.

Cowie, P. A. & Scholz, C. H. 1992c. Growth of faults by accumulation of seismic slip. *J. geophys. Res.* **97**, 11085–11095.

Dawers, N. H., Anders, M. H. & Scholz, C. H. 1993. Growth of normal faults: displacement–length scaling. *Geology* **21**, 1107–1110.

Ellis, M. A. & Dunlap, W. J. 1988. Displacement variation along thrust faults: implications for the development of large faults. *J. Struct. Geol.* **10**, 183–192.

Gillespie, P. A., Walsh, J. J. & Watterson, J. 1992. Limitations of dimension and displacement data for single faults and the consequences for data analysis and interpretation. *J. Struct. Geol.* **14**, 1157–1172.

Larsen, P.-H. 1988. Relay structures in a Lower Permian basement-involved extension system, East Greenland. *J. Struct. Geol.* **10**, 3–8.

Muraoka, H. & Kamata, H. 1983. Displacement distribution along minor fault traces. *J. Struct. Geol.* **5**, 483–495.

Peacock, D. C. P. 1991. Displacements and segment linkage in strike-slip fault zones. *J. Struct. Geol.* **13**, 1025–1035.

Peacock, D. C. P. & Sanderson, D. J. 1991. Displacements, segment linkage and relay ramps in normal fault zones. *J. Struct. Geol.* **13**, 721–733.

Peacock, D. C. P. & Sanderson, D. J. 1994. Geometry and development of relay ramps in normal fault systems. *Bull. Am. Ass. Petrol. Geol.* **78**, 147–165.

Pollard, D. D. & Segall, P. 1987. Theoretical displacements and stresses near fractures in rock: with applications to faults, joints, veins, dikes and solution surfaces. In: *Fracture Mechanics of Rock* (edited by Atkinson, B. K.). Academic Press, London, 277–349.

Scholz, C. H., Dawers, N. H., Yu, J. Z., Anders, M. H. & Cowie, P. A. 1993. Fault growth and fault scaling laws: preliminary results. *J. geophys. Res.* **98**, 21951–21961.

Sibson, R. H. 1989. Earthquake faulting as a structural process. *J. Struct. Geol.* **11**, 1–14.

Walsh, J. J. & Watterson, J. 1987. Distributions of cumulative displacement and seismic slip on a single normal fault. *J. Struct. Geol.* **9**, 1039–1046.

Walsh, J. J. & Watterson, J. 1988. Analysis of the relationship between displacements and dimensions of faults. *J. Struct. Geol.* **10**, 239–247.

Williams, G. & Chapman, T. 1983. Strains developed in the hanging-walls of thrusts due to their slip/propagation rate: a dislocation model. *J. Struct. Geol.* **5**, 563–571.